analytical chemistry

Article

pubs.acs.org/ac

Numerical Modeling of Solid-Phase Microextraction: Binding Matrix Effect on Equilibrium Time

Md. Nazmul Alam,[†] Luis Ricardez-Sandoval,[‡] and Janusz Pawliszyn*[,†]

[†]Department of Chemistry and [‡]Department of Chemical Engineering, University of Waterloo, Waterloo, Ontario N2L 3G1, Canada

Supporting Information

ABSTRACT: Solid-phase microextraction (SPME) is a well-known sampling and sample preparation technique used for a wide variety of analytical applications. As there are various complex processes taking place at the time of extraction that influence the parameters of optimum extraction, a mathematical model and computational simulation describing the SPME process is required for experimentalists to understand and implement the technique without performing multiple costly and time-consuming experiments in the laboratory. In this study, a mechanistic mathematical model for the processes occurring in SPME extraction of analyte(s) from an aqueous sample medium is presented. The proposed mechanistic model was validated with previously reported experimental data from three different sources. Several key factors that affect the extraction kinetics, such as sample agitation, fiber coating thickness, and presence of a binding matrix component, are discussed. More interestingly, for the first time, shorter or longer equilibrium times in the presence of a binding matrix component were explained with the help of an asymptotic analysis. Parameters that contribute to the variation of the equilibrium times are discussed, with the assumption that one binding matrix component is present in a static sample. Numerical simulation results show that the proposed model captures the phenomena occurring in SPME, leading to a clearer understanding of this process. Therefore, the currently presented model can be used to identify optimum experimental parameters without the need to perform a large number of experiments in the laboratory.

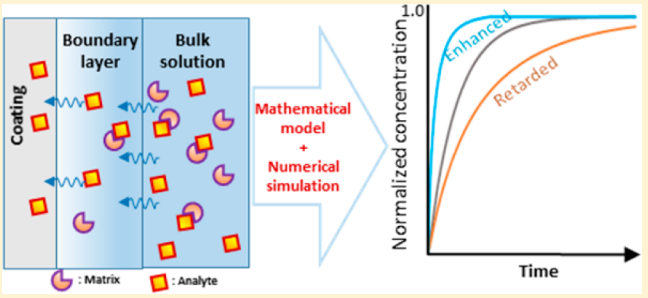

Solid-phase microextraction (SPME) has already been recognized by the scientific and industrial community as a powerful alternative sampling and sample preparation technique to technologies such as liquid–liquid or solid-phase extraction, as is evidenced by its rapid growth in recent decades.[1] The theory and practice of SPME have been examined in considerable detail in recent years in order to facilitate the processes of learning and application of this relatively new technique.[2] In SPME, a small amount of extracting material (usually polymeric) is dispersed onto a solid support to create an open-bed extraction phase. When the solid-supported extraction medium is exposed to an analytical sample for a period of time, the extraction yield is primarily dependent on the partitioning of analyte(s) between the sample bulk phase and the supported extraction phase. The partitioning is, in turn, dominated by physicochemical factors related to the analyte, the sample matrix (i.e., the part of sample other than the analyte), and the extraction phase. Based on the total residence time of the extraction phase in the sample solution, two extraction methods are used: (i) equilibrium extraction, which refers to extractions that take place when the extraction amount does not change significantly or when partition equilibrium is reached, and (ii) nonequilibrium extraction, which is the extracted amount at any given time before a state of equilibrium is reached. The extraction processes in SPME consist of several physical domains with several processes occurring simultaneously: diffusion, convection, matrix binding, and adsorption or absorption.[3] Different research groups have proposed slightly different approaches to model the kinetics of the absorption process for SPME. For example, some groups[4,5] considered the SPME fiber as a one-compartment, first-order kinetic model, whereas our group[2] divided the uptake process into two parts: intrafiber molecular diffusion in the coating domain and mass transfer around the fiber, which is governed by intralayer molecular diffusion over a stagnant layer with a finite thickness. Hermens and co-workers[6] modified the latter approach by introducing the mass transfer coefficient as a leading force due to the concentration gradient between bulk medium and fiber surface. Nevertheless, all these models have been simplified such that an analytical solution for the proposed model can be obtained; this can cause difficulties for experimentalists seeking to implement them in developing practical SPME methods that can be realistically applied to actual systems. Moreover, quantification of freely dissolved analytes with SPME under nonequilibrium conditions can be erroneous due to the influence of matrix components in the kinetic regime of extraction.[7] Some studies reported an increased analyte uptake rate in the presence of matrix during the kinetic phase of extraction.[8] The plausible

Received: June 13, 2015
Accepted: September 7, 2015
Published: September 7, 2015

DOI: 10.1021/acs.analchem.5b02239
Anal. Chem. 2015, 87, 9846–9854

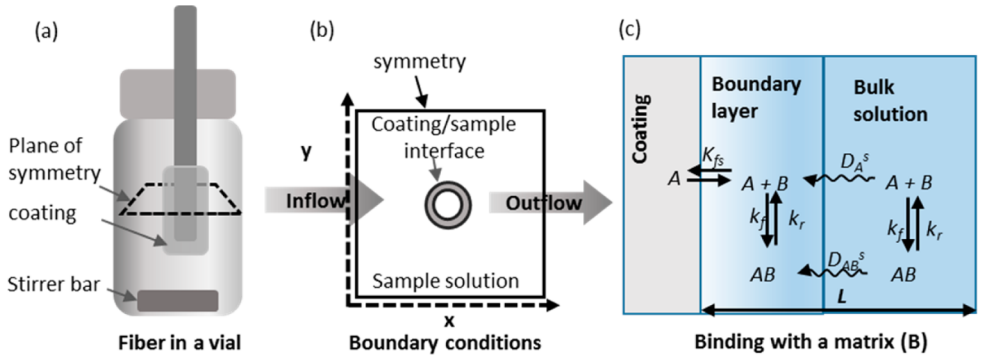

Figure 1. Schematic representation of the SPME/sample configuration. (A) Experimental geometry based on Louch et al.,[12] containing a magnetic stirrer-mediated convection. Here a silica rod is used as a support for the coating, which is immersed in a sample solution for direct extraction. (b) Two-dimensional geometry with the boundary conditions used in the model. (c) Schematic diagram of the transport processes occurring in each region in the presence of a binding matrix component (B). An analyte (A) binds with B with forward (k_f) and reverse (k_r) rate constants. Both free and bound analytes can diffuse to the boundary layer with diffusivities D_A^s and D_{AB}^s, respectively. It is assumed that only the analyte can be absorbed into the coating with a distribution constant of K_{fs}.

explanation for this enhanced kinetics is known as the "diffusion layer effect".[7] Conversely, other studies reported unaltered uptake kinetics in the presence of matrix.[9] Although the majority of the reports agree with the fact that the matrix can affect the uptake kinetics only if the extraction is limited by the diffusion in the boundary layer, a lack of understanding remains regarding the effect of physical parameters on transport kinetics in a complex matrix.

In spite of all the developments achieved in different aspects of SPME, from creation of different formats to expansion of applications, it still remains a challenge for experimentalists to readily determine suitable experimental conditions that can provide acceptable (optimal) extraction amounts at low analyte concentrations. As such, the development of a computational model will help increase our current knowledge of SPME methods by providing insight into the nature and dynamic characteristics of the extraction process[10] In addition, the utilization of a computational model would significantly decrease the time and labor needed to develop and test several SPME designs as compared to the current practice of performing multiple (expensive) experiments.

In this work, a computational-based mechanistic model for the absorption processes occurring in SPME has been developed by use of the finite element analysis software Comsol Multiphysics. Several common SPME experimental parameters, such as effect of agitation, fiber coating thickness, and presence of a binding matrix component, were considered and tested with the proposed model. The mechanistic model presented in this study is able to provide insight into how physical parameters affect the extraction kinetics of an analyte from a binding matrix component-containing sample. A set of general guiding principles that were adapted from an asymptotic analysis[11] were used as a predictive tool to achieve desired uptake kinetics or to explain the experimental extraction time profile for a complex matrix. The mechanistic model was validated with previously published experimental data obtained from different sources.

EXPERIMENTAL SECTION

Mathematical Model. The present model involves three simultaneous and coupled processes: fluid flow past the SPME fiber dipped in the sample to be analyzed, mass transport to and from the fiber coating, and absorption of analyte by the fiber coating. Each of the domains considered in the present model is described next.

In the present mechanistic model, a typical geometry of SPME sampling was set up based on the experimental configurations reported by Louch et al.,[12] where the sample was placed in a vial stirred with a magnetic stirrer, which provided convective flow, and the SPME fiber was inserted through the vial cap. A schematic representation of the sample vial and SPME fiber, along with the corresponding modeling domain, is depicted in Figure 1a. The fiber was located away from the center of the vial in order to avoid the central vortex region and to satisfy the assumption that the fluid flows past the fiber with a velocity normal to the fiber axis.[13] The present analysis assumes a simple 2D geometry (Figure 1b) for simplicity of modeling and in order to reduce the amount of necessary calculations. The xy plane is set to be the cross section of the sample container, whereas the x-axis is set to be along the direction of flow. The governing equations for fluid flow, mass transport, and matrix effect are described next.

Fluid Flow Equations. Since the flow in the sampling container of SPME is in a low Reynolds number condition, it is assumed to be a laminar flow. The Navier–Stokes equation was employed to model the fluid flow in the sampling container. The conservation of momentum for incompressible fluid flow in a 2D geometry can be formulated as follows:

$$\rho\frac{\partial u}{\partial t} + \rho\left(u\frac{\partial u}{\partial x} + v\frac{\partial u}{\partial y}\right) - \mu\nabla^2 u + \frac{\partial p}{\partial x} = 0 \quad (1)$$

$$\rho\frac{\partial v}{\partial t} + \rho\left(u\frac{\partial v}{\partial x} + v\frac{\partial v}{\partial y}\right) - \mu\nabla^2 v + \frac{\partial p}{\partial y} = 0 \quad (2)$$

where u and v are the velocity components in the x and y directions, respectively; ρ is fluid density, p is pressure, and μ is fluid viscosity. For incompressible fluid flows, the following continuity equation is also considered:

$$\frac{\partial u}{\partial x} + \frac{\partial v}{\partial y} = 0 \quad (3)$$

Boundary conditions for the fluid flow model are shown in Figure 1b. Symmetry conditions ($\partial u/\partial x = \partial v/\partial y = 0$) were set at the two edges (Figure 1b). The boundary condition at the outlet was set to $p = 0$. A linear velocity was set at the inlet of

DOI: 10.1021/acs.analchem.5b02239
Anal. Chem. 2015, 87, 9846–9854

the geometry. In order to obtain the linear velocity from stirring the solution with a magnetic stir bar, the following equation was employed:[2]

$$u(x) = 0.575\pi NR^2\frac{1}{x} \tag{4}$$

where R is the radius of the stir bar and N represents the revolutions per second.

Mass Transport Equations. The analyte is transported by diffusion and convection in the bulk solution, whereas diffusion is the only transport mechanism occurring in the fiber coating. According to Fick's law, the following mass balances can be formulated to describe the time-dependent mass transport model for the present system:[14]

$$\frac{\partial C_A{}^s}{\partial t} + \nabla(-D_A{}^s\nabla C_A{}^s + C_A{}^sU) = 0 \tag{5}$$

$$\frac{\partial C_A{}^f}{\partial t} + \nabla(-D_A{}^f\nabla C_A{}^f) = 0 \tag{6}$$

where $C_A{}^s$ and $C_A{}^f$ denote the concentrations (moles per cubic meter) of analyte A in solution phase and fiber coating, respectively. $D_A{}^s$ and $D_A{}^f$ are the diffusivity coefficients (square meters per second) in solution phase and in the fiber coating, respectively, while U denotes the velocity field, which can be obtained from the Navier−Stokes model described in the previous section. Equation 5 is valid for the solution side where convection is applied, whereas eq 6 is for the fiber's domain, where only diffusion is assumed to occur. At the coating/solution boundary, the conditions that ensure continuity of the dependent variables in the two regions, that is, fiber coating and aqueous solution, need to be specified.[15] As schematically shown in Figure S1 in Supporting Information, the fluxes at the boundary are coupled by use of Newton's law-type expressions:

$$-D_A{}^f\frac{\partial C_A{}^f}{\partial x} = M(C_A{}^s - K_{fs}C_A{}^f) \tag{7}$$

$$-D_A{}^s\frac{\partial C_A{}^s}{\partial x} = M(K_{fs}C_A{}^f - C_A{}^s) \tag{8}$$

where M is an arbitrary parameter called the stiff-spring velocity term, which should be of a large enough value so that a considerable mass exchange between the two regions can be established. This technique has been used in previous studies that consider mass transfer between two different media.[16,17] K_{fs} is called the partition coefficient. When a liquid phase is in contact with a solid phase, K_{fs} can be defined as the ratio of concentration of a species in the solid phase to that in the liquid phase where they come in contact ($K_{fs} = C_A{}^f/C_A{}^s$).[2]

A specified inlet concentration equal to the initial concentration was set at the inlet boundary ($C_A{}^s = C_A{}^{s,0}$) and vanishing of $\partial C_A{}^s/\partial x^2$ at the outlet. The following equality of the mass flux of the analyte was considered at the sample vessel wall:

$$(C_A{}^sU - D_A{}^s\nabla C_A{}^s) = 0 \tag{9}$$

Equations for Binding Matrix Component. When a binding matrix component is present (e.g., humic organic matter in a water sample), association and dissociation between the freely dissolved analytes and the binding matrix in the sample domain can be expressed as follows:

$$A + B \rightleftarrows AB$$

where A is the freely dissolved analyte, B represents the binding matrix component, and AB is the bound species. The present study assumes that the fiber coating absorbs only analytes in a matrix-containing sample and follows the same physics as described in the previous section for mass transport equations. In the solution domain, simple binding kinetics between analyte and matrix were used to model the influence of the matrix on extraction of analyte (i.e., second-order forward and first-order backward).[18] The modeled experimental systems involved addition of bovine serum albumin or humic acids to water samples, as previously reported in the literature.[19,20] The model parameters used in this study are shown in Table S1 in Supporting Information. Transport of the species in the sample is schematically shown in Figure 1c.

The rates of association (k_f) and dissociation (k_r), commonly expressed as the dissociation constant (K_D), determine the strength of the affinity interaction in eq 11, which regulates analyte release from the bound matrix into the sample medium:

$$K_D = \frac{k_r}{k_f} = \frac{C_AC_B}{C_{AB}} \tag{11}$$

Here C_A, C_B, and C_{AB} are the molar concentrations of free analyte in the sample, free matrix component (e.g., humic acid), and bound matrix component, respectively.

Mass transport within the sample can be described by use of mass balances for free analyte and analyte-bound matrix component. The concentration of free analyte (C_A) at the diffusion boundary layer changes with respect to diffusion from the sample as well as association or dissociation with the bound matrix:

$$\frac{\partial C_A}{\partial t} = \nabla(D_A\nabla C_A) - k_fC_A(C_{B,T} - C_{AB}) + k_rC_{AB} \tag{12}$$

where $C_{B,T}$ is the concentration of total matrix added.

The concentration of complex (C_{AB}) relies only on equilibrium binding:

$$\frac{\partial C_{AB}}{\partial t} = k_fC_A(C_{B,T} - C_{AB}) + k_rC_{AB} \tag{13}$$

where the concentration of free binding matrix (C_B) is described as the difference between the concentration of total matrix added ($C_{B,T}$) and the concentration of complex (C_{AB}):

$$C_B = C_{B,T} - C_{AB} \tag{14}$$

Computational Model. COMSOL Multiphysics 4.4, a finite element method (FEM) based software package, was used in this study to analyze mass transfer processes in SPME. In order to obtain an accurate representation of the SPME system, the time-dependent partial differential equations for each of these physical processes must be solved simultaneously. The procedure used to solve this problem is divided into two steps: (1) determination of the fluid velocity profile at steady state, with the assumption of incompressible flow, and (2) use of this steady-state velocity profile as the initial condition to solve for the coupled transient mass transport and absorption equations. The extracted amount at each time point was calculated by multiplying the average concentration in the fiber by its volume. The normalization of extracted amount was carried out by dividing the extracted amount at each time point by the equilibrium quantity.

DOI: 10.1021/acs.analchem.5b02239
Anal. Chem. 2015, 87, 9846−9854

RESULTS AND DISCUSSION

Model Validation. *Effect of Convection on Equilibrium Time.* The mechanistic model developed in this study has been validated with previous experimental work performed by our group for the extraction of benzene from an aqueous solution by a polydimethylsiloxane (PDMS) coating.[12] The model developed in this study can predict the equilibration time with the absence or presence of stirring in the sample solution (shown in Figure 2).The model slightly underestimates the extracted amount for the static condition. Unavoidable convection due to fiber or solution movement might contribute to the higher extracted amount at each time point. To further validate the model for static conditions, a full equilibration time profile for static conditions was shown to be well-fitted as presented in Figure S2. The equilibration time, 100 s, predicted by the present model is in agreement with the experimental data presented in a previous study[12] for stirring speed of 2500 rpm. Moreover, the simulated results for varying coating thicknesses provided very good fitting with the experimental data, as shown in Figure S3. The good fitting of the experimental data indicates the coupling between solution and coating phases in the mathematical model for both agitated and nonagitated sample systems.

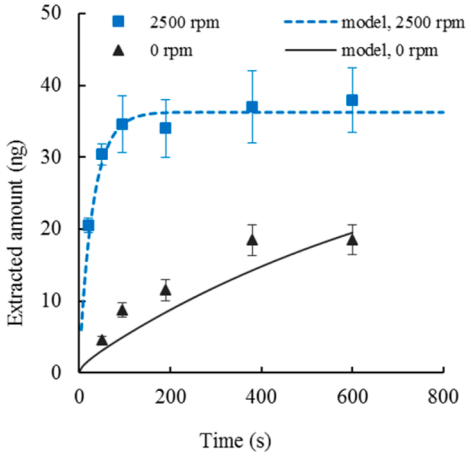

Figure 2. Effect of stirring on the extraction profile of 1 ppm benzene in water extracted with a 56 μm thick PDMS coating. Here $D_A^s = 1.08 \times 10^{-9}$ m^2/s, $D_A^f = 2.8 \times 10^{-10}$ m^2/s, $C_A^s = 1$ ppm, and $K_{fs} = 125$. The error bars represent standard deviations ($n = 3$).

Matrix Effect on Equilibrium Time. The matrix effect on SPME equilibrium time is still not well understood. Here, the proposed mathematical model is employed to explain the mechanism of the kinetics of extraction in the presence of a binding matrix component in sample. The assumption was made that no significant physical adsorption or partition of matrix components occurs on the surface of the coating. In order to test whether the model can reproduce experimental data for shorter or unaltered equilibrium time, two different experimental setups were considered. First, the model was validated with experimental data reported by Hermens and co-workers[19] on the effect of bovine serum albumin (BSA) on uptake kinetics of pyrene from an aqueous sample by use of a PDMS fiber coating. The experimental and simulated data are shown in Figure 3a. The model predicted the experimental data very well, even at different concentration levels of albumin. In this experimental setup, the equilibrium time was shorter for increased concentrations of albumin. Another validation of the model is shown in Figure 3b, with the experimental data obtained from Broeders et al.[20] The proposed model has been shown to predict experimental data when the time to reach equilibrium was not perturbed, while the extracted amount at equilibrium was less in the presence of matrix (albumin) than that of the standard chlorpromazine (analyte) sample. Details on the rate of extraction influenced by the presence of a binding matrix component are discussed in detail in the following section.

Mechanisms of Matrix Effects on Equilibrium Time. A literature review indicates that possible binding matrix effect on SPME kinetics fall into three different categories. The most common is reduced equilibrium time, which is particularly problematic when the goal is to measure the freely dissolved concentration under nonequilibrium conditions. In other words, calibration of SPME under nonequilibrium conditions would be possible only if the binding matrix containing the sample to be analyzed and the calibration sample (without binding matrix) had identical uptake dynamics. The reduction of equilibration time was typically observed where the amount of analyte extracted by the coating was negligible (usually less

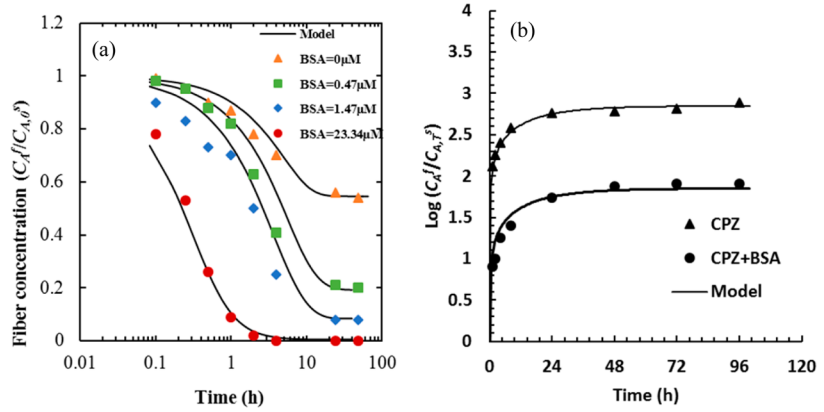

Figure 3. Influence of a binding matrix component (BSA) on equilibration time. (a) Experimental data from Hermens and co-workers[19] were fitted with the developed model. Here, both the equilibration time and extracted amount were influenced by the presence of albumin in pyrene extraction by PDMS-coated fiber. (b) Model simulation fitted with data from Broeders et al.[20]. Here, only the extraction amount was influenced by the presence of BSA during the extraction of chlorpromazine (CPZ) by polyacrylate coating. The model parameters are presented in Supporting Information (Table S1).

DOI: 10.1021/acs.analchem.5b02239
Anal. Chem. 2015, 87, 9846−9854

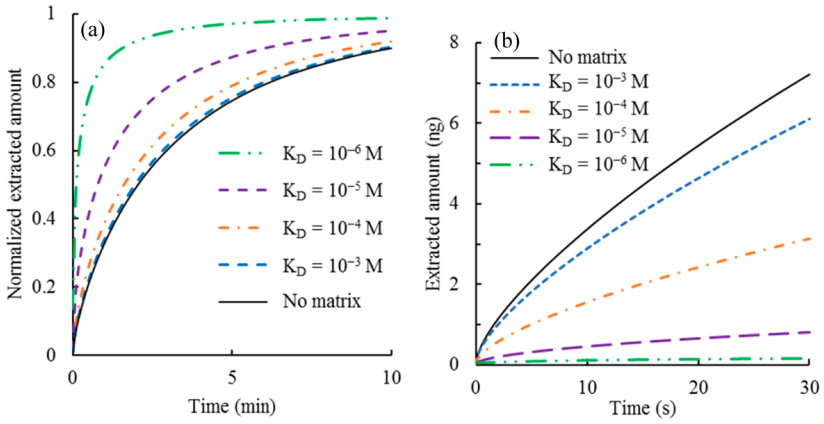

Figure 4. (a) Model simulation of equilibrium time profiles, influenced by varying the strength of the binding matrix from weak ($K_D = 10^{-3}$ M) to strong ($K_D = 10^{-6}$ M), for a chlorpromazine to BSA ratio of 1:2.5. (b) Extracted amount at initial stage of extraction time profiles. For this study, k_f was kept constant at 1×10^6 $M^{-1}{\cdot}s^{-1}$ and k_r varied to obtain different K_D values. For all values of k_f and k_r, $\beta \gg 1$ and $\gamma \ll 1$. Analyte depletion was assumed to be negligible (less than 5%) by setting radius of the sampling container (L) at 10 mm which is equivalent to 15 mL of the sample. Moreover, the convection was set to 0 (static conditions) to assume only diffusion-controlled transport of analyte. All other model parameters are presented in Table S1.

than 5%) compared to the initial amount present in the sample, that is, the depletion was negligible.[7] The second class of binding matrix effect observed was with sampling systems where a significant quantity of analyte was depleted from the sample solution. While the rate of extraction becomes slower in the binding matrix-containing sample, the extracted amount is almost the same compared to the standard sample.[21] The third class of binding matrix effect pertains to an initial fast extraction followed by a slower rate, which increases the equilibration time with significantly lower extracted amount at equilibrium.[22] With the help of an asymptotic analysis,[11] these three possible scenarios can be described by the present model and are explained next.

To explain the effects of a binding matrix component on uptake kinetics, the physical process of transport under the condition of diffusion-limited extraction is described by considering the following three dimensionless parameters. α represents the amount of freely dissolved analyte (C_A) at the beginning of the experiment relative to the total amount of binding matrix ($C_{B,T}$):

$$\alpha = \frac{C_A}{C_{B,T}}$$

This term is influenced by K_D of the analyte−matrix pair, since the system is assumed to be initially at equilibrium; therefore, α represents a measure of free analyte in the sample matrix.

The second parameter, β, relates the time scale of analyte diffusion to the time scale of unbinding of the analyte−matrix complex:

$$\beta = \frac{L^2 k_r}{D_A^s}$$

This term is dependent on size of the sample container (L), dissociation rate of the complex (k_r), and diffusivity of the analyte through the sample (D_A^s).

The third parameter, γ, is the concentration of bound matrix component in the sample relative to the unbound portion at the beginning of the experiment:

$$\gamma = \frac{k_f C_A}{k_r} = \frac{C_A}{K_D}$$

For $\gamma \gg 1$, most of the binding matrix component is in the bound state initially. Conversely, if $\gamma \ll 1$, only a small fraction of the binding matrix component has bound analytes. This term is governed by K_D and the amount of free analyte at the beginning of an experiment.

Scenario 1: Shorter Equilibrium Time and Diffusion-Controlled Kinetics. At first, the diffusion-controlled kinetics of SPME was established by increasing the diffusivity of the analyte in the solution and observing the concomitant changes in extraction time profiles (Figure S4 in Supporting Information). An increase in analyte diffusivity in the solution, from 1×10^{-9} to 5×10^{-6} m^2/s, yielded a substantially faster uptake rate, which supports the diffusion-controlled kinetics hypothesis. All the kinetic studies presented in the following sections were carried out under the condition of diffusion-controlled kinetics.

Effect of K_D on Uptake Kinetics. In order to study the effect of different parameters on extraction, an experimental system using chlorpromazine binding to BSA was considered,[20] where the equilibrium dissociation constant (K_D) was calculated as 5.4×10^{-4} M. K_D is a measure of binding strength between the analyte and the binding matrix; generally, the higher the hydrophobicity (higher log P), the lower the K_D value for the analyte−binding matrix complex. Please note that a PDMS coating was assumed instead of using a polyacrylamide coating, as the present scenario aims to study extraction under the diffusion-controlled regime. The mathematical model was used to investigate the effect of K_D on extraction kinetics, since the kinetics are not sensitive to changes in individual values of k_f and k_r (Figure S5 in Supporting Information). The effect of K_D was studied by varying k_r while keeping k_f constant, since the rate of association tends to be more consistent between binding pairs than the rate of dissociation. Figure 4a shows that the kinetics of extraction is influenced by the strength of the analyte−matrix pair (K_D). Interestingly, K_D values of 10^{-5} and 10^{-6} provided the most significant enhancement in this study. The asymptotic analysis provided that under the conditions of diffusion-controlled kinetics, that is, fast decomplexation ($\beta \gg$

DOI: 10.1021/acs.analchem.5b02239
Anal. Chem. 2015, 87, 9846−9854

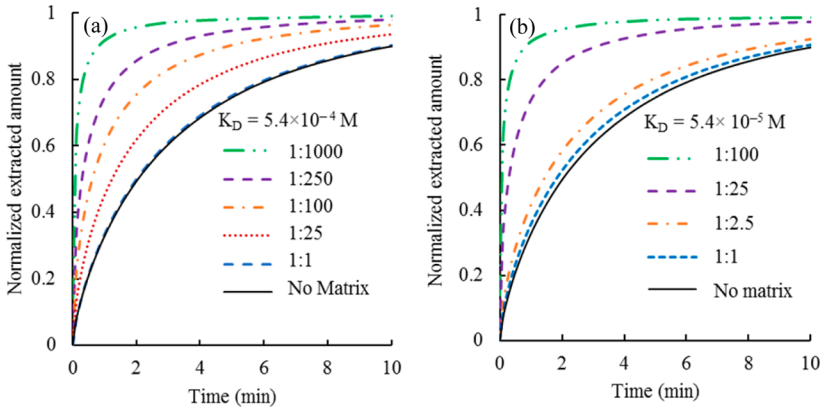

Figure 5. Effect of the ratio of analyte (chlorpromazine) to binding matrix component (BSA) on the extraction kinetics. (a) For weak binding complex, the ratio was varied from 1:1000 to 1:1. (b) For strong binding complex, the ratio was varied from 1:100 to 1:1. Here, the extent of kinetic enhancement is positively influenced by the strength of the binding partners. Model parameters are presented in Table S1. The convection was set to 0 (static conditions).

1) and with a small proportion of bound matrix component ($\gamma \ll 1$), extraction occurs on a single time scale (t_s), according to

$$t_s = \frac{L^2(1 + C_{B,T}/K_D)}{D_A{}^s} \quad (15)$$

This term demonstrates that equilibrium time is dependent on hydrophobicity of the analyte at constant values of $C_{B,T}$, L, and $D_A{}^s$. Increasing hydrophobicity under these conditions will lead to a decrease in equilibration time. The model predicts that a weak interaction (10^{-3} M) does not appreciably affect the equilibration time (equilibrium reached at 20 min), whereas a strong interaction (10^{-6} M) significantly reduced the time needed to reach equilibrium to only 5 min. A weak binding matrix component does not appreciably perturb the kinetics under these conditions, although the conditions $\beta \gg 1$ and $\gamma \ll 1$ pertained in all cases. It is worthwhile to mention that with the increase in K_D, increasing amount of analyte remains bound to the matrix and therefore the quantity of free analyte becomes less.

In contrast to the above findings, extraction time profiles at the early stages of extraction show that the uptake rate for analyte solution without binding matrix component is the highest (Figure 4b). The rate also decreases as the binding strength between the analyte and matrix increases. Although the initial uptake rate for sample solution without matrix is the highest, it takes the longest time to reach equilibrium (shown in Figure 4a). We assume that with the decease of free analyte concentration in solution, due to progressively stronger binding affinity toward the binding matrix, the fiber coating requires lesser amount of analyte to reach equilibrium. For instance, when K_D is equal to 10^{-5} or 10^{-6}, the binding matrix buffers the system, leading to very low free analyte concentration and consequently reducing the equilibration time. Moreover, the concentration gradient in solution domain extends a shorter distance for the high K_D values, whereas a thicker gradient is obvious for solution free of binding matrix, as the complex located close to the coating provides the required amount of analyte to reach conditions close to equilibrium value (Figure S6). Therefore, equilibration time becomes shorter for samples containing binding matrix compared to extraction from matrix-free solution, when the concentration is equal to the free concentration in solution containing the binding matrix component.

Effect of Analyte to Binding Matrix Component Ratio on Equilibrium Time. The mathematical model was used to examine the effect of the ratio of initial analyte to binding matrix component (for example, BSA), containing both weak and strong binding, on the reduction of equilibration time. In this case, the analyte concentration was held constant while the BSA concentration was varied. As shown in Figure 5a, for the weak binding complex system ($K_D = 5.4 \times 10^{-4}$ M), the simulation results show that an increase in analyte to BSA ratio from 1:25 to 1:1000 provides a 25% reduction of equilibration time. For the strong binding complex system ($K_D = 5.4 \times 10^{-5}$ M), shown in Figure 5b, a similar range of reduction is achieved with an increase in ratio from only 1:2.5 to 1:100. This phenomenon can be analyzed with the time scale according to eq 15. If $C_{B,T}/K_D \ll 1$, then the equilibration time is independent of both matrix concentration and K_D. Therefore, the concentration of binding matrix component must be greater than K_D for shorter equilibrium time to obtain. In other words, at a lower ratio of analyte to binding matrix component, the equilibrium time is barely affected by the matrix, but the effect becomes pronounced as the ratio increases. This also supports the findings from a study of different K_D values, presented in the previous section, that the shorter equilibration time is due to the extraction of less free analytes to attain equilibrium. Ramos et al.[23] reported that the binding matrix (humic acids) did not interfere with determination of the freely dissolved concentration of hydrophobic organics under nonequilibrium SPME with a PDMS coating. Oomen et al.[24] indicated that this observed result might be due to the use of a very low concentration of matrix in the experiment, which produced a lower concentration of bound matrix than that of free analytes. The present mechanistic model with the asymptotic analysis quantitatively explained the required conditions for influencing equilibrium time.

Scenario 2: Retarded Uptake Rate and Diffusion-Controlled Kinetics. A decrease in uptake rate or longer equilibrium time has been observed in cases where the uptake is still controlled by the diffusion of analyte in solution. However, in such cases, the freely dissolved analyte is locally depleted in the diffusion boundary layer due to the higher amount of extraction by the fiber; that is, local depletion is significant. In that case, analytes need to diffuse from longer distances for the system to reach equilibrium. Poerschmann et al.[21] reported a retardation in the uptake rate after addition of humic or fulvic

DOI: 10.1021/acs.analchem.5b02239
Anal. Chem. 2015, 87, 9846−9854

acid to a water sample with organotin compounds; that is, the time to reach equilibrium was increased. Similarly, a retardation of uptake kinetics is observed when smaller sample volumes and lower concentrations of analyte are used compared to the capacity of the SPME coating. For instance, Reyes-Garces et al.[22] reported slow uptake rates for some moderately hydrophobic compounds (for example, metoprolol) in blood plasma samples. This category of binding matrix effect can be explained by the asymptotic analysis and the proposed mathematical model. This type of longer equilibrium is observed when the kinetics are controlled by diffusion ($\beta \gg 1$) and when a large proportion of the binding matrix component is bound ($\gamma \gg 1$). A two-stage extraction time profile is obtained with the initial time scale of $(L^2/D_A^s)[1 + (C_{B,T}/C_A)]$. At this stage, the extraction kinetics depends on the total binding matrix concentration ($C_{B,T}$) and the initial free analyte concentration (C_A). Dependence of the initial uptake kinetics on the concentration of free analyte is shown in Figure S7 in Supporting Information. Here the initial uptake rate increases with decreasing binding matrix component to analyte ratio, whereas the equilibration times remain the same. As the free analyte concentration is depleted until its concentration is equal to K_D, the second stage of extraction starts with a time scale of $(L^2/D_A^s)[1 + (C_{B,T}/K_D)]$ for the remaining analyte molecules present in the sample. The latter time scale is identical to the shorter equilibration time with the binding matrix discussed above in scenario 1. For the extraction time profile of sample containing binding matrix, an initial fast extraction is followed by slow diffusion-controlled conditions, compared to the one-stage and faster equilibration for the solution free of binding matrix (Figure 6). The equilibration time is governed by the

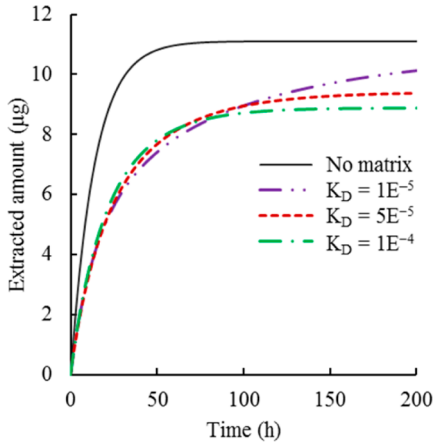

Figure 6. Two-stage extraction time profiles with initial fast uptake kinetics followed by slow kinetics in the presence of a binding matrix component, compared to the single-step and faster uptake kinetics for the solution free of binding matrix. Here C_A = 110 μM and $C_{B,T}$ = 100 μM. All other parameters are shown in Table S2. The convection was set to 0 (static conditions).

second time scale, which depends on the binding strength (K_D values) between the analyte and binding matrix component. With the increase of binding strength, the equilibrium times are clearly shown to be decreased. Furthermore, the mathematical model was employed to study the concentration profiles in solution domain at different times of extraction under static conditions (Figure S8). It is seen that the gradients are steeper for matrix-free standard analyte solution compared to the sample containing binding matrix. The concentration gradients extend throughout the vial for both sample containing binding matrix and matrix-free solution, unlike scenario 1, where the gradients are thinner for sample containing binding matrix compared to the matrix-free case (Figure S6). Therefore, the mathematical model presented here can be used to predict uptake profiles in cases where the rate is retarded by the local depletion of analyte but where the kinetics are still diffusion-controlled.

Scenario 3: Retarded Uptake Rate and Analyte Dissociation-Controlled Kinetics. In the third case, the matrix substantially reduces both the uptake rate and the extraction amount at equilibrium. This type of profile was recently reported by Reyes-Garces et al.[22] for extraction of a very hydrophobic analyte, stanozolol (K_D with human serum albumin, HSA, = 5 × 10^{-9} M) from a blood plasma sample. From the mathematical analysis and computational simulation, the condition for this scenario is that the dissociation of bound analyte from the binding matrix is slow compared to diffusion in solution; that is, $\beta \ll 1$ or $(1/k_r) \gg (L^2/D_A^s)$. Any free analyte produced by dissociation of the analyte−matrix pair is negligible compared to the existing freely dissolved analytes in the sample solution. As shown in Figure 7, nearly all the freely

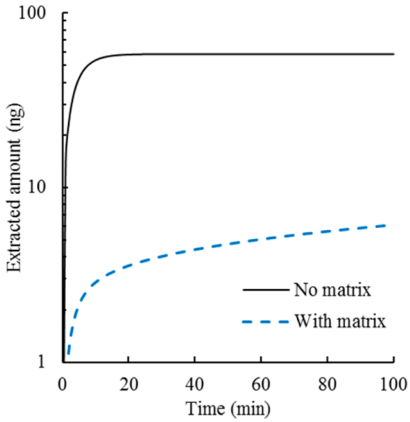

Figure 7. Retardation of uptake kinetics controlled by L^2/D_A^s in the initial stage followed by the slower stage governed by dissociation of analyte from the bound matrix component (k_r), compared to the single-stage and faster kinetics in the absence of binding matrix. Here K_D = 5 × 10^{-9} M, C_A = 5.1 μM, $C_{B,T}$ = 100 μM, and L = 1 mm. All other parameters are presented in Table S3. The convection was set to 0 (static conditions).

dissolved analyte is extracted by the coating over the diffusion time scale, L^2/D_A^s. The initial fast diffusive uptake is followed by slow dissociation of bound analytes over the time scale of $1/k_r$. The uptake rate in the latter stage increases with faster dissociation of analyte from the binding matrix (see Figure S9a). Since analyte diffusivity through environmental or biological samples does not change significantly, either k_r or L needs to be modified for our computational sample system to observe this type of slow kinetics. It is more feasible to modify the diameter of the sample container than the binding kinetics. If the diameter is kept constant at 10 mm, as in the previous simulation experiments, a k_r of <10^{-4} s^{-1} is required for $\beta \approx 1$. This translates to a bound matrix with a half-life of ∼3 h. However, if the vial diameter is sufficiently decreased, it is possible to achieve $\beta \ll 1$ for physically relevant k_r values. More precisely, in order to observe the unbinding-controlled dynamics, the diameter L would need to be below the order

DOI: 10.1021/acs.analchem.5b02239
Anal. Chem. 2015, 87, 9846−9854

of $(D_A^s/k_r)^{1/2}$. It was also found that the slower uptake rate is dependent on the extraction capacity of the coating (K_{fs}) when the value of k_r is kept constant (Figure S9b, Supporting Information).

The information provided by the above analysis can be used to design an experimental setup with desired extraction time profiles. In scenario 1, the rate of analyte extraction decreases smoothly over a single time scale. In scenarios 2 and 3, there are two distinct time scales: an initially fast uptake rate, followed by a more gradual uptake rate. The two time scales in scenario 2 are related, as they are both proportional to L^2/D_A^s, whereas the two time scales in scenario 3 are independently controlled by L^2/D_A^s and k_r, as long as $\alpha \gg \beta\gamma/(\gamma + 1)$ and $L \ll (D_A^s/k_r)^{1/2}$. Another key difference between scenarios 2 and 3 is that all of the bound analyte molecules remain in the bound state throughout the fast mode for scenario 3, while approximately half the bound analyte molecules undergo unbinding in the initial fast stage for scenario 2. Thus, the complex sample system can influence not only the time scales of extraction but also the amounts of analyte extracted in each stage.

CONCLUSIONS

The present work presented a mechanistic-based mathematical model that describes the uptake kinetics in SPME of analytes from either a binding matrix-free standard solution or a matrix-containing solution. The proposed mathematical model provided excellent prediction of the experimental data available in the literature. The majority of discussion was limited to static conditions, but the conclusions are analogous to cases involving convection. In the case when convection (e.g., stirring) is present, mass transfer is controlled by diffusion in the boundary layer formed close to the coating surface, not in the whole vial, as demonstrated in the static case where the boundary layer is equivalent to the size of the vial. It should be emphasized that agitation level will determine the mass transfer rates and the equilibrium value, but in this contribution we focused on binding matrix effects exclusively, as they are poorly understood. It was not clear under what experimental conditions the uptake rate is altered with the presence of a binding matrix in sample solution. Now, with the help of this mathematical model and computational simulation, one can easily determine whether the presence of a binding matrix can alter the equilibrium time, based on the physicochemical properties of analyte and matrix, as well as the choice of SPME coating. The modeling has demonstrated that the decrease in equilibration time is not due to increased rate of extraction but to the requirement of less extracted amount to reach equilibrium when binding matrix is present. Overall, the simulation results obtained for the present analysis have shown that the present model is a reliable and relatively inexpensive practical method of characterizing the performance of SPME. This model can be used for sample matrices containing one type of analyte binding component. However, for biomedical applications such as human blood or tissue sampling with SPME, further improvement of the model to describe multicomponent phenomena is needed. We are currently extending this study to the application of SPME extraction in tissue or blood sampling. In addition, the good agreement between experimental results and modeling indicates that determination of binding constants and associated kinetics can be obtained from experimental data by appropriate fit of calculated values.

ASSOCIATED CONTENT

Supporting Information

The Supporting Information is available free of charge on the ACS Publications website at DOI: 10.1021/acs.analchem.5b02239.

Parameters used for fitting experimental data, coating/solution interface boundary conditions, effect of coating thickness on kinetics, test for boundary layer controlled diffusion, concentration gradients in solution domain, and effect of binding rate constants and partition constants on uptake kinetics (PDF)

AUTHOR INFORMATION

Corresponding Author

*Phone 1-519-888-4567, ext 84641; fax 1-519-746-0435; e-mail janusz@sciborg.uwaterloo.ca.

Notes

The authors declare no competing financial interest.

ACKNOWLEDGMENTS

This work was supported by the Natural Sciences and Engineering Research Council of Canada and the Premier Discovery Award. We are thankful for initial suggestions on this project from Wennan Zhao and Zhipei Qin from the Department of Chemistry, University of Waterloo.

NOMENCLATURE

M	stiff-spring velocity
C_A^s	analyte concentration in solution
k_f	association rate constant
k_r	dissociation rate constant
K_{fs}	partition coefficient
D_A^s	diffusion coefficient of analyte in solution
D_A^f	diffusion coefficient of analyte in fiber
C_B	concentration of unbound matrix component
D_{BS}	diffusion coefficient of the complex in solution
ρ	density of water
μ	dynamic viscosity of water
R	radius of magnetic stirrer
L	radius of sample container
t_s	time scale of analyte diffusion

REFERENCES

(1) Boyaci, E.; Rodriguez-Lafuente, A.; Gorynski, K.; Mirnaghi, F.; Souza-Silva, E. A.; Hein, D.; Pawliszyn, J. *Anal. Chim. Acta* **2015**, *873*, 14−30.

(2) Pawliszyn, J. *Solid Phase Microextraction: Theory and Practice*; Wiley−VCH: New York, 1997.

(3) Lao, W.; Maruya, K. A.; Tsukada, D. *Anal. Chem.* **2012**, *84*, 9362−9369.

(4) van Eijkeren, J. C. H.; Heringa, M. B.; Hermens, J. L. M. *Analyst* **2004**, *129*, 1137−1142.

(5) Vaes, W. H. J.; Ramos, E. U.; Hamwijk, C.; van Holsteijn, I.; Blaauboer, B. J.; Seinen, W.; Verhaar, H. J. M.; Hermens, J. L. M. *Chem. Res. Toxicol.* **1997**, *10*, 1067−1072.

(6) Heringa, M. B.; Hogevonder, C.; Busser, F.; Hermens, J. L. M. *J. Chromatogr. B: Anal. Technol. Biomed. Life Sci.* **2006**, *834*, 35−41.

(7) Heringa, M. B.; Hermens, J. L. M. *TrAC, Trends Anal. Chem.* **2003**, *22*, 575−587.

(8) Kopinke, F. D.; Ramus, K.; Poerschmann, J.; Georgi, A. *Environ. Sci. Technol.* **2011**, *45*, 10013−10019.

(9) Heringa, M. B.; Pastor, D.; Algra, J.; Vaes, W. H. J.; Hermens, J. L. M. *Anal. Chem.* **2002**, *74*, 5993−5997.

DOI: 10.1021/acs.analchem.5b02239
Anal. Chem. 2015, 87, 9846−9854

(10) Santillo, M. F.; Ewing, A. G.; Heien, M. L. *Anal. Bioanal. Chem.* **2011**, *399*, 183−190.
(11) Vulic, K.; Pakulska, M. M.; Sonthalia, R.; Ramachandran, A.; Shoichet, M. S. *J. Controlled Release* **2015**, *197*, 69−77.
(12) Louch, D.; Motlagh, S.; Pawliszyn, J. *Anal. Chem.* **1992**, *64*, 1187−1199.
(13) Mahmud, T.; Haque, J. N.; Roberts, K. J.; Rhodes, D.; Wilkinson, D. *Chem. Eng. Sci.* **2009**, *64*, 4197−4209.
(14) Bird, R. B.; Stewart, W. E.; Lightfoot, E. N. *Transport Phenomena*, 2nd ed.; Wiley & Sons: New York, 2002.
(15) Datta, A.; Rakesh, V. *An Introduction to Modeling of Transport Processes*, 1st ed.; Cambridge University Press: New York, 2010.
(16) Buchwald, P. *Theor. Biol. Med. Modell.* **2009**, *6*, 5.
(17) Ellis, J. S.; Strutwolf, J.; Arrigan, D. W. *Phys. Chem. Chem. Phys.* **2012**, *14*, 2494−500.
(18) Crank, J. *The Mathematics of Diffusion*. 2nd ed.; Oxford University Press: Oxford, U.K., 1975.
(19) Kramer, N. I.; van Eijkeren, J. C. H.; Hermens, J. L. M. *Anal. Chem.* **2007**, *79*, 6941−6948.
(20) Broeders, J. J.; Blaauboer, B. J.; Hermens, J. L. M. *J. Chromatogr., A* **2011**, *1218*, 8529−8535.
(21) Poerschmann, J.; Zhang, Z.; Kopinke, F. D.; Pawliszyn, J. *Anal. Chem.* **1997**, *69*, 597−600.
(22) Reyes-Garces, N.; Bojko, B.; Pawliszyn, J. *J. Chromatogr., A* **2014**, *1374*, 40−49.
(23) Ramos, E. U.; Meijer, S. N.; Vaes, W. H. J.; Verhaar, H. J. M.; Hermens, J. L. M. *Environ. Sci. Technol.* **1998**, *32*, 3430−3435.
(24) Oomen, A. G.; Mayer, P.; Tolls, J. *Anal. Chem.* **2000**, *72*, 2802−2808.

DOI: 10.1021/acs.analchem.5b02239
Anal. Chem. 2015, 87, 9846−9854